Impact of Structure Relaxation on the Ultimate Performance of a Small Diameter, n-Type ⟨110⟩ Si-Nanowire MOSFET

Gengchiau Liang, *Member, IEEE*, Diego Kienle, Sunil K. R. Patil, Jing Wang, *Member, IEEE*, Avik W. Ghosh, and Sanjay V. Khare

***Abstract*—We investigate the impact of structure relaxation on the upper performance of a silicon nanowire metal-oxide-semiconductor field-effect-transistor (MOSFET) with small diameter employing a semiclassical transport model to calculate its ballistic I-V characteristics. For wires along the ⟨110⟩ axis and 1 nm diameter, structure relaxation induces large changes in the bond length of silicon atoms at the surface (∼ 33%). Despite these bond length variations, the effect of reconstruction on the ballistic ON-current of Si-NW MOSFETs turns out negligible in the case considered, which can be attributed to an only slight variation of the electron effective mass after reconstruction.**

***Index Terms*—Bandstructure, field-effect transistor (FET), geometry optimization, nanowire, quantum confinement, tight binding.**

I. Introduction

SILICON nanowires (NWs) have attracted much attention by the device and circuit engineering community due to their potential applications as metal-oxide-semiconductor field-effect-transistors (MOSFETs) [1] and nanosensors [2]. To explore the ultimate performance limit of NW MOSFETs as well as the physics of nanosensors, the study of the transport properties of Si-NWs is a first important step, for which their electronic bandstructure is a key ingredient. To calculate their E-k dispersion, empirical tight-binding (TB) methods such as $sp^3d^5s^*$ orbital TB have been used recently to calculate their electronic structure [3]. As long as the atomic structure remains undistorted, an $sp^3d^5s^*$ orthogonal TB model is a good starting point to understand the NW-electronic structure of unrelaxed nanowires. It is well-known, however, that the surface of a semiconducting material such as Si reconstructs due to rebonding of the surface dangling bonds and causes the geometry to reconstruct within the first few layers of the wire. To what extent these structural relaxations affect the performance of nanodevices is still an open question.

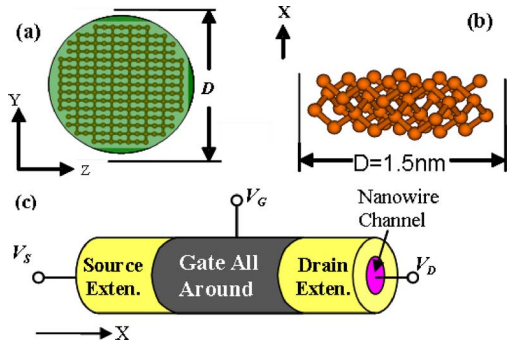

Fig. 1. Schematic diagram of a simulated Si nanowire MOSFET. (a) Cross section of a ⟨100⟩ oriented cylindrical Si nanowire. (b) Unit cell of the NW shown in (a). (c) Schematic diagram of the nanowire MOSFET.

To approach this problem one needs an electronic structure method which can deal with structurally deformed systems and can handle bulk and surface properties simultaneously. Among the class of semi-empirical approaches, Extended Hückel Theory (EHT) stands out due to its transferability and flexibility to handle bulk and defect geometry as well [4]. The EHT approach has been widely used in the chemistry community to understand the electronic structure of molecules [5], and has been recently extended to describe the bandstructure of bulk solids [6], [7]. Due to the transferability of EHT-parameters, the respective bulk-parameters can be applied to free surfaces as well as to determine the surface electronic structure of reconstructed Si(100)-(2×1) [7], [8].

In this work, we use EHT to explore the electronic structure of a Si nanowire along ⟨110⟩ and ⟨100⟩ direction with circular cross section. Fig. 1(a) and (b) shows the schematic diagram of the wire geometry, whose structure is used to be optimized by *ab initio* calculations. The impact of the structural relaxation on the I-V characteristics of n-type Si-NW MOSFETs, cf. Fig. 1(c), is studied using a semiclassical top-of-the-barrier model for transport in the ballistic limit [9]. For a small diameter cylindrical Si-NW (1 nm), the initial result shows that relaxation plays an important role in the NW geometry causing 33% structural change. However, the ballistic ON-current of a n-channel Si-NW MOSFET is reduced only slightly due to a small change in the conduction band (CB)-effective mass after relaxation.

Manuscript received June 10, 2006; revised September 8, 2006. This work was supported in part by the MARCO Focus Center on Materials, Structures, and Devices, in part by DURINT, in part by the National Centre for Supercomputing Applications, in part by Ohio Supercomputer, in part by the University of Toledo, in part by the Defense Advanced Research Projects Agency (DARPA), and startup grants from UVA. The review of this paper was arranged by Associate Editor R. Lake.

G. Liang, D. Kienle, and J. Wang are with the School of Electrical and Computer Engineering, Purdue University, West Lafayette, IN 47907 USA (e-mail:elelg@nus.edu.sg; kienle@ecn.purdue.edu).

S. K. R. Patil is with the Department of Mechanical, Industrial and Manufacturing Engineering, University of Toledo, Toledo, OH 43606 USA.

A. W. Ghosh is with the School Electrical and Computer Engineering, University of Virginia, Charlottesville, VA 22904 USA.

S. V. Khare is with the Department of Physics and Astronomy, University of Toledo, Toledo, OH 43606 USA.

Color versions of one or more of the figures in this paper are available online at http://ieeexplore.ieee.org.

Digital Object Identifier 10.1109/TNANO.2007.891816

II. Approach

To investigate how structure relaxation affects the ultimate device performance of a Si-NW MOSFET, cf. Fig. 1(c), we first optimize the bulk-like structure of a cylindrical Si-NW without H passivation, cf. Fig. 1(a) and (b), using density functional theory (DFT) within the local density approximation (LDA) [10]. After geometry optimization, the SiNW surface is H-passivated to saturate dangling bonds. This structure is then used to calculate within EHT the electronic E-k dispersion using $\mathrm{sp^3d^5}$-orbitals for each Si-atom. Finally, the E-k dispersion is used to obtain the self-consistent I-V characteristics of the Si-NW FETs using a semiclassical "top-of-the-barrier" MOSFET model for ballistic transport.

A. Geometry Optimization

For the initial geometry, we use the structure of a bulk terminated nanowire without H passivation with the minimum periodic unit along a specific direction such as $\langle 110 \rangle$ in this study. These initial atomic positions are relaxed using first-principles total energy calculations based on DFT-LDA and use the Vienna Ab Initio Simulation Package (VASP) for this purpose [11]–[14]. Core electrons are implicitly treated by ultra-soft Vanderbilt type pseudopotentials [14] as supplied by Kresse and Hafner [15]. This *ab initio* method uses a supercell approach with periodic boundary conditions along the three Cartesian axes. The wires from the initial geometry are rotated so that their axes are along the Z direction of the supercell. To separate a single wire from its images we use a sufficiently large vacuum domain along the X and Y axes to render interaction negligible. Systematic tests show that a 24 Å vacuum region along both X and Y axes is adequate. For each calculation, irreducible k-points are generated according to the Monkhorst–Pack scheme [16]. The single-particle wave functions are expanded in a plane-wave basis using a 240 eV kinetic energy cutoff. Tests using a higher plane-wave cutoff and a larger k-point sampling indicate that a numerical convergence better than ± 1.0 meV is achieved for relative energies. All atoms are allowed to relax until a force tolerance of 0.008 eV/Å is reached for each atom. Convergence is achieved when the change in total energy of the system between two ionic iterations is below 1.0 meV. After convergence the positions of the relaxed atoms are used for bandstructure calculations, as described in the next section.

B. Electronic Bandstructure Calculations

To calculate the electronic structure of nanosystems such as Si-NWs, we employ Extended Hückel Theory (EHT) which also allows us to passivate surfaces by physically attaching chemical species such as hydrogen atoms to the Si-surface atoms to remove dangling bonds. The surface boundary conditions are, therefore, fully controlled by the Si-H bonding chemistry and the environment at the interface. Fig. 2 demonstrates how the dangling bond states within the bandgap [Fig. 2(a)] are completely removed after H passivation [Fig. 2(b)]. In EHT, the Hamiltonian of a Si nanowire is constructed—based on its atomic structure—from the basis-function overlap between

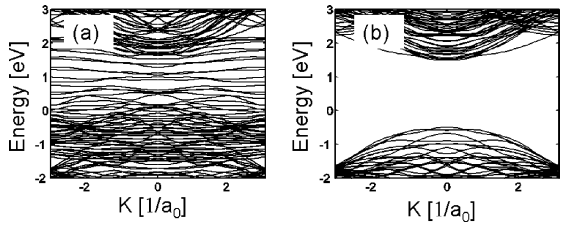

Fig. 2. 1-D bandstructure of a Si-NW with cylindrical cross section and $\langle 100 \rangle$ orientation. (a) Without hydrogen passivation of the wire surface, cf. Fig. 1(a), the entire bandgap is filled with surface states due to dangling bonds. (b) After H passivation, the DB-states are removed from the gap region and the original bandgap is recovered.

Si-atoms. Since the basis functions for each Si-atom are known explicitly [6], the overlap matrix S_{ij} between any two basis functions, ϕ_ι and ϕ_j, can be calculated

$$S_{ij} = \langle \phi_i | \phi_j \rangle \,. \tag{1}$$

The Hamiltonian is determined by employing the EHT principle [5]

$$H_{ij} = 0.5 K_{\mathrm{EHT}}\, S_{ij}(H_{ii} + H_{jj}) \tag{2}$$

where $H_{ii/jj}$ is the on-site energy of atom i, j, and K_{EHT} is an additional parameter usually set to 2.3 for silicon atoms and 1.75 for hydrogen atoms. Once the transport direction is specified, the diameter D of the nanowire, its shape, and unit cell can be defined, cf. Fig. 1(b). The overlap matrix and Hamiltonian of atoms within the unit cell and atoms within neighbor unit cells are obtained from (1) and (2). We denote these two terms as S_l and H_l, respectively, where l is the unit cell index with $l = 0$ for the center unit cell and $l \neq 0$ for the lth nearest-neighbor cell. The overlap matrix and Hamiltonian in 1-D k-space is calculated by taking the Fourier transform

$$\begin{aligned} H_{k_m} &= \sum_l H_l \exp[-j \cdot k_m (z_l - z_0)] \\ S_{k_m} &= \sum_l S_l \exp[-j \cdot k_m (z_l - z_0)] \end{aligned} \tag{3}$$

where $k_m = m\pi/L$ is the wave vector within the first Brillouin zone and L is the periodicity of the 1-D lattice. $z_l = lL$ and refers to the unit cell position. Due to the nonorthogonality of the EHT basis sets, a generalized eigenvalue problem, $H_{k_m}\Psi = ES_{k_m}\Psi$, has to be solved for each k_m within the first Brillouin zone. Fig. 2 shows the electronic structure of a cylindrical Si-NW with $\langle 100 \rangle$ axis and $D = 1.5$ nm: (a) without and (b) with H passivation. As shown in Fig. 2(a), the entire region inside the bandgap is covered by surface states due to unsaturated dangling bonds. These states are eliminated after H passivation, as shown in Fig. 2(b).

C. Transport Calculation

To explore bandstructure effects on the ultimate performance of Si-NW MOSFETs, we employ a semiclassical top-of-the-barrier model for transport to calculate its I-V characteristics within the ballistic limit [9]. A key quantity of this model is the

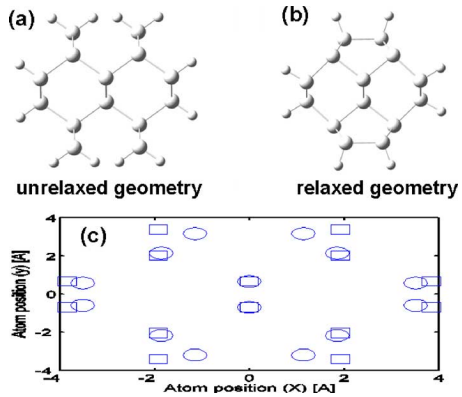

Fig. 3. Cross section of an (a) unrelaxed and (b) relaxed Si-NW unit cell with 1 nm diameter along the ⟨110⟩ axis and H-passivated surface to remove dangling bonds. After relaxation the pair of surface Si-atoms at the top and bottom, cf. Fig. 3(b), become connected. (c) Y-X plot of the atomic positions of the Si-atoms for the (a) unrelaxed (square) and (b) reconstructed geometry (circles). The maximum change in the bond length is $\sim 33\%$ after structure relaxation.

number of mobile carriers at the top-of-the-barrier (N), which is directly computed from the previously determined E-k

$$N = \int_{-\infty}^{\infty} \frac{dk}{\pi} [f(E(k)+U_{scf}-E_{fs})+f(E(k)+U_{scf}-E_{fs}+qV_D)] \tag{4}$$

where $f(E)$ is the Fermi function and E_{fs} is the chemical potential in the source region. Equation (4) is self-consistently coupled to Poisson's and Laplace's equation to obtain the effective potential $U_{scf} = U_P + U_L$ at the top-of-the-barrier. The Laplace potential U_L is determined from a simplified capacitance model which incorporates the capacitance of the gate insulator (C_G), the drain (C_D), and the source terminal (C_S), respectively. For the Poisson part, we employ a simple charging model with $U_P = U_0 N$, where U_0 is the single charging energy [9].

In this work, we assume for simplicity perfect gate control, i.e., $C_G \gg C_D$, and C_S to focus on the impact of relaxation effects. Once N and U_{scf} are converged, the current is evaluated using the semiclassical transport equation in the ballistic limit [9]

$$I = \frac{2q}{h} \int_{U_{scf}}^{\infty} dE[f(E-E_{fs}) - f(E-E_{fs}+qV_D)]. \tag{5}$$

III. Results

Fig. 3(a) shows the bulk-like cylindrical ⟨110⟩ silicon nanowire with $\mathrm{D} = 1$ nm with H passivation to eliminate the dangling bonds. Similarly, Fig. 3(b) shows the structure of the reconstructed Si-NW with hydrogen attached to its surface, as described in Section II. The effect of the structure relaxation is evident through the rebonding of the silicon atoms at the top and bottom of the wire surface, cf. Fig. 3(b). Fig. 3(c) compares the X-Y positions of the silicon atoms before (square) and after relaxation (circle). As can be seen, atoms close to the center of the unit cell shift slightly, while the maximum deviation in bond length ($\sim 33\%$) appears for the surface atoms after surface reconstruction.

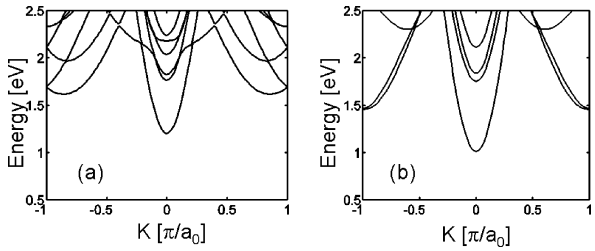

Fig. 4. E-k dispersion of the CBs for: (a) an unrelaxed and (b) relaxed Si-NW along the ⟨110⟩ and geometry, as shown in Fig. 3(a) and (b). The CB effective mass extracted by a parabolic fit, respectively, the bandgap at the Γ–point is in case: (a) $m = 0.11m_0$, $E_G = 2.4$ eV, and (b) $m = 0.12m_0$, $E_G = 2.0$ eV.

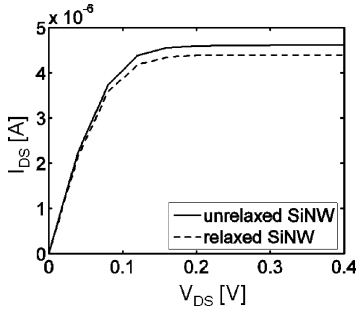

Fig. 5. I-V characteristics of a ⟨110⟩ Si-NW MOSFETs with 1 nm diameter and 0.75 nm oxide thickness within the ballistic limit at gate bias $\mathrm{V}_{GS} = 0.4$ V. The saturation current I_{DS} for the relaxed wire (dashed) is slightly decreased compared with the undistorted one (solid).

Fig. 4 shows the E-k relation for the CBs of: (a) an unrelaxed and (b) a relaxed Si-NW for the geometries shown in Fig. 3(a) and (b), respectively. For a better comparison, we have aligned the E-k dispersions with respect to the middle of the bandgap. We find that some material properties strongly depend on these geometries. For example, the NW bandgap decreases from 2.4 eV (unrelaxed) to 2.0 eV (relaxed). The electron effective mass at the Γ-point, however, remains almost constant from $0.11m_0$ to $0.12m_0$ after relaxation [17]. A qualitative reason for the decrease in E_G is that the surface atoms increase the number of their bonding Si-atoms after relaxation. Hence, these surface atoms are closer to bulk-like Si-atoms with a smaller, more bulk-like Si bandgap (1.2 eV). To confirm this hypothesis, our study of the electronic structure of Si-nanowires needs to be extended further.

To compare the ultimate performance of a n-type ⟨110⟩ Si-NW MOSFET in its ON-state for the two different geometries, we first assume that the gate has perfect control on the electrostatic potential at the top-of-the-barrier along the entire channel, as shown in Fig. 1(c). The equivalent oxide thickness (EOT) is set to 0.75 nm. Afterwards, we fix the OFF-current density to 0.11 $\mu\mathrm{A}/\mu\mathrm{m}$ according to the 40 nm node of the 2005 ITRS report [18] by tuning the gate work function in each case. Using the semiclassical model, the calculated I_{DS} versus V_{DS} characteristics at $V_{GS} = 0.4$ V is shown in Fig. 5. We find only a small reduction of the ON-current for an n-type Si-NW MOSFET after surface reconstruction. However, if we assume that the same type of metal for the gate is used in both cases (work function of the gate is not allowed to change), we find

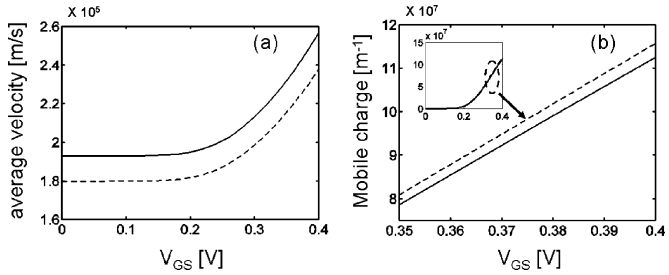

Fig. 6. (a) Average carrier velocity versus V_{GS} at $V_{DS} = 0.4$ V for a $\langle 110 \rangle$ Si-NW MOSFETs with $D = 1$ nm with relaxed (dashed line) and unrelaxed (solid line) geometry. (b) Respective mobile charge in the wire channel versus V_{GS} for the same bias conditions as in (a).

that due to the smaller bandgap of the reconstructed wire, the respective transistor has a smaller threshold voltage (V_T), but larger OFF-current which in turn degrades the I_{ON}/I_{OFF} ratio.

To gain further insight into the device performance of this Si-NW MOSFET, we determine the electron average velocity and the number of mobile carriers, as shown in Fig. 6(a) and (b) as a function of the gate bias V_{GS}. At $V_{DS} = 0.4$ V, the average velocity for the unrelaxed Si-NW MOSFET with $D = 1$ nm is higher than for the relaxed one, cf. Fig. 6(a). This characteristics can be qualitatively explained within an effective mass approximation of the conduction band where the carrier velocity $v \propto 1/\sqrt{m^*}$. Since the effective mass of the unrelaxed wire is smaller than of the relaxed one, the respective velocity is higher, as shown in Fig. 6(a). The mobile carrier density (n) depends linearly on the effective device capacitance (C), which consist of a parallel combination of the geometric capacitance (C_Σ) and the so-called quantum capacitance (C_Q) defined as $d(q^2N)/d(-U_{scf})$ [9]. For "large" devices such as traditional Si MOSFETs, $C_Q \gg C_\Sigma$, the device capacitance is dominated by the geometric capacitance, so that the charge density should depend on C_Σ, and (V_{DD}-V_T). For nanosize devices, however, the quantum capacitance can become comparable to the geometric capacitance, so that C_Q plays an increasingly important role in controlling the density of mobile carriers. As shown in Fig. 6(b) at $V_{DS} = 0.4$ V, the carrier density n of the relaxed and unrelaxed NW are now different due to the different bandstructure effective masses for the two cases. This difference implies that these two NW devices belong to the intermediate regime where effects due to the quantum capacitance cannot be ignored. As a result, the impact of the carrier velocity variation on the ON-current ($I = qnv$) of the Si-NW MOSFET would be suppressed, cf. Fig. 5, and becomes independent on the effective mass variation in the limit $C_\Sigma \gg C_Q$.

To gain a more detailed insight in the device degradation of Si-NW MOSFETs, the model should be extended by incorporating 3-D electrostatics along with the real space charge distribution in the device, as well as scattering processes, such as surface roughness scattering [19]. Our assumption that electron transport is ballistic enables us to investigate the upper performance of Si-NW MOSFETs. Surface roughness scattering in small diameter Si-NW MOSFETs would only play a less important role in decreasing the ON-current and, thus, lowering further the performance than in planar MOSFETs [19].

IV. Conclusion

We investigate for the first time relaxation effects on the I-V characteristics of a small diameter, n-type $\langle 110 \rangle$ Si-NW MOSFET within the ballistic limit. Further study is needed to investigate the influence of surface states and their passivation chemistry on the threshold voltage of the channel. Although significant variations in the structure with respect to bond length are found ($\sim 33\%$), the respective saturation current shows only a small decrease due to a slight increase in the CB-effective mass after structure relaxation. Studies to further investigate the orientation, as well as the size dependence of structure relaxation on the performance of ballistic p-type, as well as n-type Si-NW FETs are in progress.

Acknowledgment

The authors acknowledge the Network for Computational Nanotechnology (NCN) for computational support. The authors would also like to thank M. Lundstrom for helpful discussions.

References

[1] Y. Cui, Z. H. Zhong, D. L. Wang, W. U. Wang, and C. M. Lieber, "High performance silicon nanowire field effect transistors," *Nano Lett.*, vol. 3, pp. 149–152, Feb. 2003.
[2] Y. Cui, Q. Q. Wei, H. K. Park, and C. M. Lieber, "Nanowire nanosensors for highly sensitive and selective detection of biological and chemical species," *Science*, vol. 293, pp. 1289–1292, Aug. 2001.
[3] J. Wang, A. Rahman, A. W. Ghosh, G. Klimeck, and M. Lundstrom, "Performance evaluation of ballistic silicon nanowire transistors with atomic-basis dispersion relations," *Appl. Phys. Lett.*, vol. 86, p. 093113, Feb. 2005.
[4] D. Kienle, J. I. Cerda, and A. W. Ghosh, "Extended Hückel theory for bandstructure, chemistry and transport. I. Carbon nanotubes," *J. Appl. Phys.*, vol. 100, p. 043714, 2006.
[5] J. N. Murrell and A. J. Harget, *Semi-Empirical Self-Consistent-Field Molecular Orbital Theory of Molecules*. New York: Wiley, 1972.
[6] J. Cerda and F. Soria, "Accurate and transferable extended Hückel-type tight-binding parameters," *Phys. Rev. B*, vol. 61, p. 7965, 2000.
[7] D. Kienle, K. H. Bevan, G.-C. Liang, L. Siddiqui, J. I. Cerda, and A. W. Ghosh, "Extended Hückel theory for bandstructure, chemistry, and transport. II. Silicon," *J. Appl. Phys.*, vol. 100, p. 043715, 2006.
[8] G.-C. Liang and A. W. Ghosh, "Identifying contact effects in electronic conduction through C60 on silicon," *Phys. Rev. Lett.*, vol. 95, p. 076403, 2005.
[9] A. Rahman, J. Guo, S. Datta, and M. Lundstrom, "Theory of ballistic nanotransistors," *IEEE Trans. Electron. Devices*, vol. 50, pp. 1853–1864, Sep. 2003.
[10] P. Hohenberg and W. Kohn, "Inhomogeneous electron gas," *Phys. Rev. B*, vol. 136, p. B864, 1964.
[11] G. Kresse and J. Hafner, "*Ab initio* molecular dynamics for liquid metals," *Phys. Rev. B*, vol. 47, p. RC558, 1993.
[12] G. Kresse, "*Ab initio* Molekular Dynamik für flüssige Metalle," Ph.D. dissertation, Technische Universiät, Wien, Austria, 1993.
[13] G. Kresse and J. Furthmüller, "Efficiency of *ab initio* total energy calculations for metals and semiconductors using a plane-wave basis set," *Comput. Mat. Sci.*, vol. 6, p. 15, 1996.
[14] D. Vanderbilt, "Soft self-consistent pseudopotentials in a generalized eigenvalue formalism," *Phys. Rev. B*, vol. 41, p. 7892, 1990.
[15] G. Kresse and J. Hafner, "Norm-conserving and ultrasoft pesudopotential for first-row and transition-elements," *J. Phys. C: Cond. Mat.*, vol. 6, p. 8245, 1994.
[16] H. J. Monkhorst and J. D. Pack, "Special points for Brillouin-zone integrations," *Phys. Rev. B*, vol. 13, p. 5188, 1976.
[17] T. Vo, A. J. Williamson, and G. Galli, "First principles simulations of the structural and electronic properties of silicon nanowires," *Phys. Rev. B*, vol. 74, p. 045116, 1976.
[18] Semiconductor Industry Association, International Roadmap for Semiconductors, 2005. [Online]. Available: http://public.itrs.net/
[19] J. Wang, E. Polizzi, A. W. Ghosh, S. Datta, and M. Lundstrom, "Theoretical investigation of surface roughness scattering in silicon nanowire transistors," *Appl. Phys. Lett.*, vol. 87, p. 043101, 2005.

Gengchiau Liang (S'05–M'07) received the B.S. and M.S. degrees in physics from the National Tsinghua University, Hsinchu, Taiwan, in 1995 and 1997, respectively, and the Ph.D. degree in electrical and computer engineering from Purdue University, West Lafayette, IN, in 2005.

He was employed as a Postdoctoral Research Associate in the Department of Electrical Engineering, Purdue University, and since December 2006, he has been with the Department of Electrical and Computer Engineering, National University of Singapore, as an Assistant Professor. His research interests focus on modeling and exploring the physics of nanoscale electronic devices including molecular devices, carbon nanotube/ribbon devices, and nanowire devices.

Diego Kienle received the prediploma (B.S.) and diploma (M.S.) degree in physics from the University of Bayreuth, Bayreuth, Germany, in 1997. He did the Ph.D. thesis at the Research Center, Juelich, Germany, and received the "Dr. rer. nat." (Ph.D.) degree from the University of Saarland, Saarland, Germany, in 2001.

He was subsequently employed as Postdoctoral Researcher at the University of Saarland and later in the Department of Electrical Engineering, Purdue University until 2006. Since January 2007, he has been with Sandia National Laboratories, CA. His research interest focus on computational modeling of quantum transport through molecular and nanoscale systems such as carbon nanotubes, silicon nanowires and semi-empirical electronic structure calculations employing nonorthogonal tight-binding. His past research areas cover dynamical correlations functions of Luttinger liquids and modeling of complex polymer fluids by means of Brownian dynamics simulations with emphasis on hydrodynamic interactions.

Sunil K. R. Patil received the B.S. degree in mechanical engineering from the Jawaharlal Nehru Technological University, Hyderabad, India, in 2001. He is currently working towards the Ph.D. degree in mechanical engineering at the University of Toledo, Toledo, OH.

His research interests are in computational material sciences, computational and experimental fluid dynamics.

Jing Wang (M'05) was born in Henan Province, China, in 1979. He received the Bachelor of Engineering degree with Highest Honor from the Department of Electronic Engineering, Tsinghua University, Beijing, China, in 2001 and the Ph.D. degree in electrical and computer engineering from Purdue University, West Lafayette, IN, in 2005. His Ph.D. research, advised by Prof. M. Lundstrom, covered device physics and simulation of silicon nanowire transistors, exploration of nanoscale MOSFETs, and simulation of high electron mobility transistors (HEMTs).

In September 2005, he joined the IBM Semiconductor Research and Development Center (SRDC), Hopewell Junction, New York, as a device modeling engineer. He is the author/coauthor of over 20 peer-reviewed journal/conference papers and a book chapter. He has also co-invented three pending U.S. patents.

Dr. Wang is a member of the American Physical Society (APS).

Avik W. Ghosh received the B.S. and M.S. degrees in physics from the Indian Institute of Technology, Kanpur, and the Ph.D. degree in physics from the Ohio State University, Columbus, in 1999.

He was subsequently employed as a Postdoctoral Fellow and Research Scientist in electrical engineering at Purdue University, and is currently an Assistant Professor of Electrical Engineering at the University of Virginia, Charlottesville. His research involves modeling electronic conduction in nanoscale devices, including atomic and molecular wires, nanoscale silicon MOSFETs, hybrid silicon-molecular devices, carbon nanotubes, silicon nanowires, and quantum dots. Among his other past research activities are ultrafast optical phenomena in semiconductor heterostructures and noise-induced transport in Brownian environments.

Sanjay V. Khare received the Ph.D. degree in theoretical physics from the University of Maryland, College Park, in 1996.

He worked at the Ohio State University (1996–1999) and the University of Illinois at Urbana–Champaign (1999–2004). He is an Assistant Professor of Physics and Astronomy at the University of Toledo since 2004. His interests are in computational materials physics, surface science, and functional nanostructures. His web address is: www.physics.utoledo.edu/~khare/.